Function of the voltage gate of gap junction channels: Selective exclusion of molecules

Yang Qu and Gerhard Dahl*

Department of Physiology and Biophysics, University of Miami, School of Medicine, Miami, FL 33101

Edited by Lily Y. Jan, University of California, San Francisco, CA, and approved November 19, 2001 (received for review June 27, 2001)

Gap junction channels span the membranes of two adjacent cells and allow the gated transit of molecules as large as second messengers from cell to cell. In vertebrates, gap junctions are composed of proteins from the connexin (cx) gene family. Gap junction channels formed by most connexins are affected by transjunctional voltage. The function of the voltage gate is unclear, because substantial electrical coupling typically remains with activated gates because of the channels dwelling in subconductance rather than closed states. Here, we find in *Xenopus* oocytes expressing cx43 or cx46 that the activated voltage gate preferentially restricts the passage of larger ions, such as fluorescent tracer molecules and cAMP, while having little effect on the electrical coupling arising from the passage of small electrolytes. Thus, a conceivable physiological role of the voltage gate is to selectively restrict the passage of large molecules between cells while allowing electrical coupling.

Gap junction channels are formed by a family of proteins, the connexins, which are expressed in most tissues of an organism. Gap junction channels between contacting cells allow the passage of ions and other small molecules between the cells and thereby synchronize cells both electrically and metabolically. Molecules up to 1,000 Daltons, including all known second messengers and some endogenous metabolites, can pass through at least some connexin channels (1).

Most vertebrate gap junction channels are regulated by voltage (2), closing when a potential difference develops between the cells (Vj). However, closure is only partial. For most connexins, even a large potential difference reduces the junctional conductance over time to about 30–50% of the maximal conductance. This incomplete closure of the channels would not break the electrical continuity of the cells, thus the function of this voltage regulation is unclear.

Like other membrane channels, gap junction channels exhibit subconductance states. In some connexin channels, the probability that the channels reside in the subconductance states is increased by a voltage gradient (3, 4). It seems possible that the subconductance states have a different selective permeability than the full conductance state, such that the flux of larger molecules like second messengers is reduced. On the basis of the conductance ratios of connexin 43 (cx43) gap junction channels for different salts such as KCl, Cs aspartate, or tetraethylammonium aspartate, it has been suggested that the subconductance state could represent a slightly higher permeation barrier than the full conductance state (5). However, by using a statistical approach on the same channels, Christ and Brink (6) concluded that subconductance states do not effectively change selectivity in a physiologically meaningful manner because of their brevity of duration in relation to the full open state.

To avoid the technical problems associated with studies on complete gap junction channels, we addressed the question of a functional role of the voltage gate initially in a more amenable model system. cx46 forms regular gap junction channels. However, when cx46 is expressed in *Xenopus* oocytes, it also forms open hemichannels in the membrane without another membrane in apposition (7, 8). As expected from simple physical principles, the hemichannels have twice the conductance of the complete gap junction channels because they are half as long (3, 9, 10). Furthermore, cx46 hemichannels exhibit permeability and gating properties like those of complete gap junction channels, except the voltage dependence is somewhat more complex. A slow gating process observed in hemichannels but not in complete gap junction channels closes the hemichannel at more negative than −30 mV potential. This gate is located toward the extracellular side of the channel (4) and is thought to be part of a docking gate or loop gate, which keeps the hemichannels closed at normal membrane potentials and opens on docking of hemichannels from apposing cells. At positive potentials, the effect of voltage on hemichannels is similar to that on complete gap junction channels, including gating polarity and preferred dwelling in a subconductance state. Thus, the latter hemichannel gate likely is identical to the Vj gate of gap junction channels (3), indicating that cx46 hemichannels can be used to study voltage effects on channel permeability.

Here, we report that the action of the voltage gate (Vj gate) modifies the selectivity of gap junction channels. The transit of fluorescent test molecules and of cAMP through cx46 hemichannels and complete gap junction channels was determined quantitatively. The flux of tracer molecules was measured by fluorescence microscopy. The flux of cAMP was assayed with the cystic fibrosis transmembrane conductance regulator (CFTR) as a reporter. The flux of these molecules through cx46 hemichannels was voltage dependent and was diminished at positive holding potential compared with that at negative holding potential. Similarly, in paired oocytes, the permeability of these tracer molecules was found to be affected by Vj.

Materials and Methods

Preparation of Oocytes. Oocytes were prepared as described earlier (11). *In vitro* transcribed mRNAs (≈20 nl) were injected into *Xenopus* oocytes. The oocytes were incubated at 18°C for 18–24 h in Oocyte Ringer's Solution (OR2) with elevated Ca^{2+} concentration (5 mM) to keep the gap junction hemichannel closed. For electrophysiology recordings, oocytes were transferred to regular OR2 (in mM: 82.5 NaCl/2.5 KCl/1 $MgCl_2$/1 $CaCl_2$/1 Na_2HPO_4/5 Hepes, pH 7.5).

***In Vitro* Transcription of mRNAs.** cx46 cloned into the expression vector rSP64T was obtained from D. L. Paul (Harvard Univ., Boston) (7). cx43 mRNA was transcribed *in vitro* from a cDNA clone (12) that was modified at the 5′-end and subcloned in pGEM3Z. mRNAs were transcribed by Sp6 RNA polymerase from 10 μg of *Eco*RI- (cx46) or *Ssp*I-linearized (cx43) plasmid by using the mMessage mMachine kit (Ambion, Austin, TX). CFTR mRNA was transcribed from *Nhe*I-linearized plasmid pACF23 (13) by using the same kit. mRNAs were quantified by

This paper was submitted directly (Track II) to the PNAS office.

Abbreviations: cx, connexin; CFTR, cystic fibrosis transmembrane conductance regulator.

*To whom reprint requests should be addressed. E-mail: gdahl@miami.edu.

The publication costs of this article were defrayed in part by page charge payment. This article must therefore be hereby marked "*advertisement*" in accordance with 18 U.S.C. §1734 solely to indicate this fact.

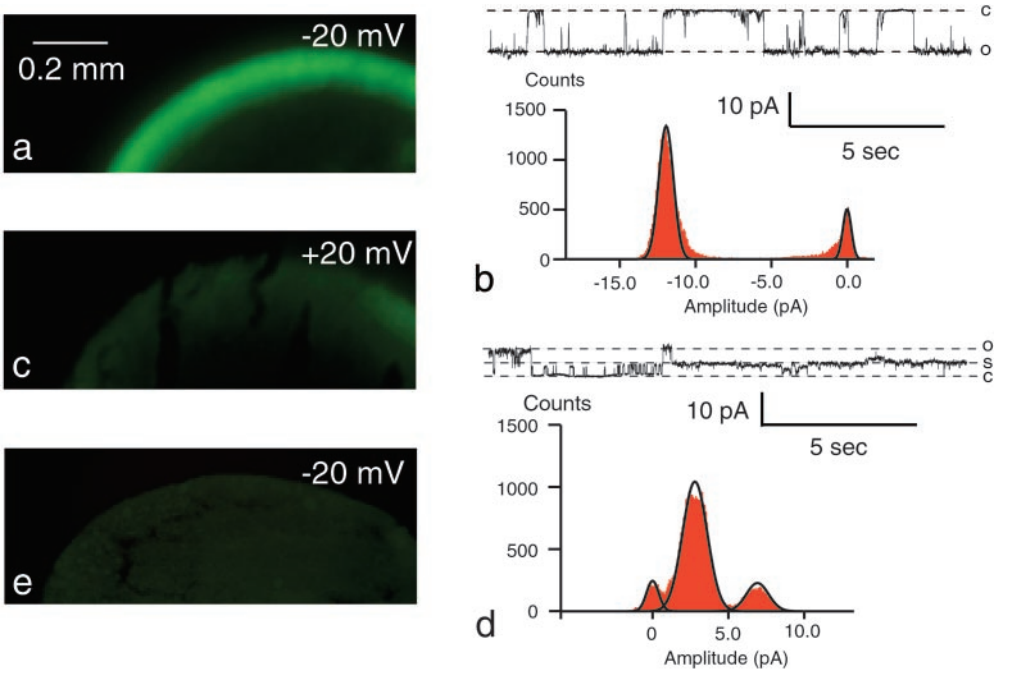

Fig. 1. Voltage-dependent uptake of calcein by oocytes expressing cx46. Calcein (1 mM) was applied to oocytes held at −20 mV (*a*) or +20 mV (*c*) for 20 min. cx46 channels were then closed by stepping the membrane potential to −80 mV and perfusing the oocytes with 5 mM calcium OR2. Oocytes were frozen and cryosectioned before viewing under a fluorescence microscope. A steep gradient of fluorescence is seen in *a* at the plasma membrane, whereas in *c* the fluorescence is at the detection threshold. Single channel records for cx46 channels at −45 mV (*b*) and at +38 mV (*d*) illustrate rectification and a subconductance as the preferred state at positive potential. To better depict the channel properties, larger potentials were chosen here. At ±20 mV, the same channel properties are seen with smaller amplitudes. *e* is an uninjected oocyte held at −20 mV while exposed to calcein for 20 min.

absorbance (260 nm), and the proportion of full-length transcripts was checked by agarose gel electrophoresis.

Fluorescent Tracer Studies. Fluorescent tracer molecules (Molecular Probes) were dissolved at 1 mM concentration in OR2. Oocytes injected with cx46 mRNA were clamped at −20 or +20 mV. Tracer molecules were applied to the oocyte in a perfusion chamber at each testing potential. The channels were closed at −80 mV immediately afterward and washed with 5 mM Ca^{2+} OR2. Oocytes were frozen in OCT compound (Miles). Cryosections (30 μm) were taken and viewed in a fluorescence microscope (Zeiss) with the filter settings appropriate for the various fluorescent tracers.

Data were analyzed with an NIH IMAGE software program (http://rsb.info.nih.gov/nih-image/). A straight line was drawn across the membrane at the place the brightest fluorescence is shown, and a profile plot was generated. In the profile plot, the area above the autofluorescence level was measured. With the time course study, the bottom line of the plotted area was fixed, and the area above the background fluorescence level was measured. The data were normalized by the membrane conductance of oocytes at −20 mV.

To ascertain that the fluorescence measurements were obtained in the linear range, various dilutions of the tracers were applied to slides carrying cryosections of unloaded oocytes of the same thickness as in the experimental conditions. Fluorescence was determined identically to the procedure described above.

Flux of cAMP. Whole cell membrane current of single oocytes was measured by using a two-microelectrode voltage clamp and recorded with a chart recorder. Both voltage-measuring and current-passing microelectrodes were pulled with a vertical Puller (Kopf Instruments, Tujunga, CA) and filled with 3 M KCl. The recording chamber was perfused continuously with solution. Membrane conductance was determined by using voltage pulses, typically of 5-s duration and of 5-mV amplitude. Voltage was stepped from a holding potential of −50 mV to a series of test potentials from −20 to +20 mV in 10-mV decrements (cx46 is closed at −50 mV and opens at −30 mV).

cx46 and CFTR mRNA mixture was coinjected into oocytes 24 h before the experiment. The recording chamber was perfused with 1 mM cAMP until the current reached the maximal state. After washing and a waiting period of 30 min, the oocyte was stepped to the next testing potential. The CFTR channel conductance was determined by subtracting the current immediately before applying cAMP from the maximal current after applying cAMP and dividing by the voltage pulse. In the control experiments, membrane current was tested at −20 and +20 mV. Oocytes were injected only with CFTR mRNA. Twenty micromolar forskolin or 1 mM cAMP was applied until the current reached the maximal state.

Junctional Conductance of cx46/43 Heterotypic Channel. cx46 and cx43 mRNA were injected into prejunctional and postjunctional cells, respectively. Approximately 24 h later, the vitelline envelope was stripped manually from the oocytes, and the two oocytes were pushed together with vegetal poles apposed (14). Junctional conductance was determined with the dual voltage clamp technique (15). Transjunctional voltages (Vj) were applied by stepping one cell over a range of −130 to +50 mV, whereas the other cell was held at −40 mV. Junctional conductance was calculated by $g_j = i_j/V_j$.

Flux of cAMP Through Heterotypic cx46/43 Channels. Oocytes were injected with either cx46 mRNA or a mixture of cx43 and CFTR mRNA. The oocytes were paired so that the cx46-expressing oocyte was the prejunctional and the cx43 and CFTR coexpressing oocyte was the postjunctional cell. Four hours after pairing,

the oocytes were voltage clamped, and the recording chamber was perfused with 1 mM cAMP until the current in the postjunctional cell reached the maximal level. After washing and a 30-min wait, the next test transjunctional voltage was applied. Using the dual voltage clamp technique, transjunctional potentials (Vj) were elicited by stepping the holding potential of the postjunctional cell (V_2) from a common holding potential ($V_1 = V_2 = -20$ mV, where V_1 is the holding potential of the prejunctional cell to a new value (V_2'). $Vj = V_1 - V_2'$. Postjunctional membrane conductance was determined by using voltage pulses of 5-s duration and 5-mV amplitude. The Cl current carried by CFTR channels in the postjunctional cell was determined by subtracting the current measured just before applying cAMP from the maximal current after applying cAMP. Membrane conductance was calculated by dividing the current by the amplitude of the test voltage pulse.

Results

Fluorescent Tracer Flux Through cx46 Hemichannels. The flux of fluorescent tracer molecules through cx46 hemichannels was determined at different potentials. Because cx46 hemichannels are open at potentials more positive to −30 mV, we used two symmetrical testing potentials, −20 and +20 mV. Oocytes expressing cx46 were exposed to fluorescent tracer molecules in the bath medium while voltage clamped to +20 or −20 mV. After exposure for 20 min, the channels were closed by negative potential (−80 mV), and elevated calcium (5 mM) and the oocytes were frozen. Tracer uptake was determined on cryosections with a fluorescence microscope. Fig. 1 shows the influx of calcein (mw 623) after a 20-min exposure. When assayed at −20 mV, the fluorescence was much brighter, and a gradient of fluorescence was seen beneath the membrane. At +20 mV, the fluorescence was near the detection threshold (compare with control, Fig. 1*e*). Single channel records of cx46 hemichannels show the predominance of a subconductance state at positive potential (Fig. 1 *b* and *d*). For clarity, current traces at larger voltages are displayed. The open probability in the range −30 to −20 mV was 0.31 (±0.12, $n = 4$) for the full open state with no significant dwell time at a subconductance state. In the range +20 to +30 mV, the open probability for the full (rectified) open state was 0.21 (±0.05) and 0.60 (±0.08) for the subconductance state in the same membrane patches.

An example of the quantitative determination of tracer uptake, in this case cascade blue, is shown in Fig. 2. The tracer uptake was determined for three time points. In all cases, the uptake was much less at +20 than at −20 mV, although the electrochemical gradient itself promotes entry at the positive potential of this negatively charged compound.

To determine whether molecular size or charge affects tracer flux at the test potentials, different fluorescent dyes (lucifer yellow, cascade blue, and calcein), all applied at 1 mM for 10 min, were tested. Calcein has the largest diameter, and cascade blue has the smallest. Fig. 3 shows a quantitative analysis; the flux of all three dyes was found to be greatly reduced at +20 mV relative to that at −20 mV, being close to the detection threshold. However, there seems to be no significant difference among three dyes at each holding potential. The macroscopic membrane conductance, on the other hand, was higher at +20 than at −20 mV (Fig. 3*b Right*) because at positive potential (+20 to +30 mV), the increased open probability counteracts the effect of the channel entering the subconductance state (see also refs. 3 and 4).

Flux of cAMP Through cx46 Hemichannels. We also tested the flux of a second messenger, cAMP, through cx46 hemichannels. In this assay, cx46 and a cAMP-activated chloride channel, CFTR, were coexpressed in *Xenopus* oocytes (Fig. 4*a*). The influx of cAMP through cx46 open hemichannels resulted in an inward current

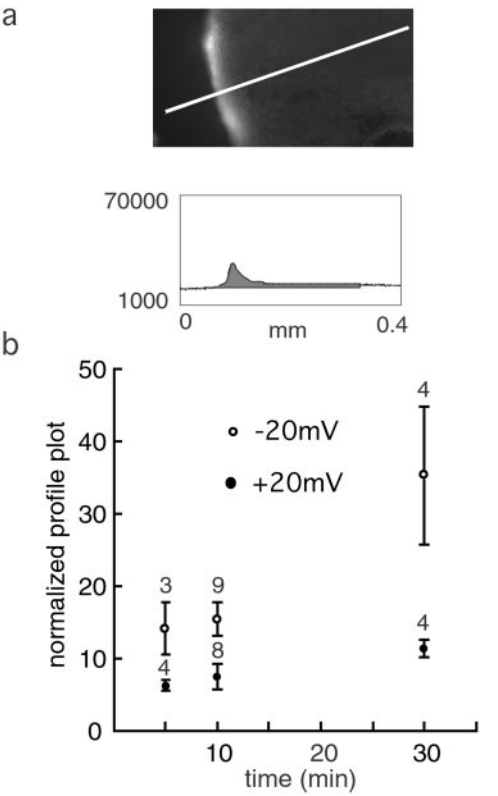

Fig. 2. Time course of uptake of cascade blue in oocytes expressing cx46. Oocytes were held at −20 mV (○) or +20 mV (●) during exposure to the fluorescent tracer for the times indicated. Fluorescence was quantitated as described in *Materials and Methods* and exemplified in *a* by generating a profile plot with NIH IMAGE software. Means ± SE are plotted, and *n* is given above the bars. For all three time points, the flux at positive and negative potentials was significantly different ($P < 0.05$).

at −20 mV and an outward current at +20 mV, consistent with a chloride current carried by CFTR (Fig. 4*b*). One millimolar cAMP applied extracellularly at −20 mV induced a large membrane conductance, as indicated by the increased currents in response to the repetitively applied 5-mV test pulses. At +20 mV, the cAMP-induced conductance change was significantly smaller (Fig. 4*b*). The average specific cAMP-induced membrane conductance at −20 mV was 80 μS, whereas at +20 mV it was 21 μS, indicating a 4-fold decrease (Fig. 4*d*).

As a control, oocytes expressing only CFTR were tested with cAMP. Surprisingly, an increase of membrane conductance was observed in the absence of endogenous cx38 channels (data not shown). Thus, the modest influx of cAMP is due either to the leakage of the cell membrane or the lesion caused by the micropipette. The elicited Cl current in this case was much smaller than that in the cx46/CFTR experiment and showed no significant difference at negative and positive holding potentials (Fig. 4*c*).

To test for direct voltage effects on CFTR channels, the same series of experiments was performed in the absence of cx46. Forskolin, a drug that is membrane permeant and increases cAMP concentration by the activation of adenylate cyclase, was used to activate CFTR channels. No significant difference was observed between the changes of membrane conductance at different holding potentials (Fig. 4*c*).

The change in membrane conductance in response to cAMP might also involve phosphorylation of cx46. To test this possibility, oocytes expressing only cx46 but not CFTR were exposed to 20 μM forskolin. No change in membrane conductance was

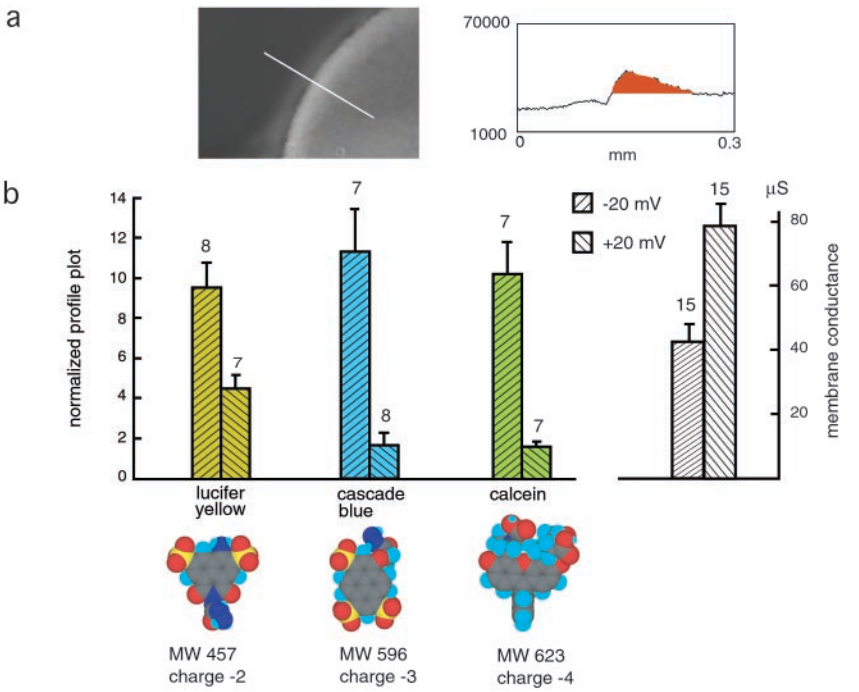

Fig. 3. Voltage-dependent uptake of lucifer yellow, cascade blue, and calcein. (*a*) Measurement of fluorescence intensity with profile blot. (*b*) Quantitative analysis of tracer flux. The fluorescence intensity data were normalized to the membrane conductance at −20 mV holding potential. Molecular models were generated with CS CHEM 3D PRO software from CambridgeSoft (Cambridge, MA). Macroscopic membrane conductance of oocytes used in this experiment at −20 and +20 mV is shown (*Right*). Means ± SE are plotted; *n* is given above the bars. The membrane conductances as well as the fluxes of all tracer molecules at positive and negative potentials were significantly different ($P < 0.01$).

observed at either −20 or +20 mV holding potentials after application of the drug (data not shown).

Flux Through Complete Gap Junction Channels. To test whether complete gap junction channels exhibit the same voltage dependence of second messenger flux as hemichannels, we adapted the CFTR assay for cell pairs (Fig. 5). Oocytes expressing cx46 were paired with oocytes expressing cx43 to form heterotypic gap junction channels. Whereas cx46 forms open hemichannels in normal oocyte Ringer solution, cx43 does not. Thus, in heterotypic pairs, cAMP can enter through the cx46-expressing oocyte and flow across the cell junction. Its appearance in the second (cx43-expressing) cell can be monitored by the coexpressed CFTR channels (Fig. 5).

The transjunctional conductance (g_j) of cx46/43 gap junction channel was tested by the dual whole cell voltage clamp technique. Both cx46 and cx43 (when paired with cx46) channels have an apparent positive gating polarity, closing when the holding potential of the cell expressing them is positive relative to the paired cell (16) (see ref. 17 for details). The voltage dependence is asymmetrical in this heterotypic channel (Fig. 6*a*), in part because the voltage sensitivity of cx46 is stronger than that of cx43 channels.

For measurement of transjunctional flux of cAMP, the prejunctional cx46-expressing cell was held at −20 mV. The postjunctional cx43-expressing cell was held at a different potential to create a transjunctional voltage. Extracellular application of cAMP resulted in the activation of a current in the postjunctional cell. This current was inward when the postjunctional cell was held at −40 mV and outward at 0 mV, consistent with a chloride current carried by CFTR. The conductance induced by cAMP in the postjunctional cell was reduced when a transjunctional voltage was applied (Fig. 6 *b* and *c*), suggesting an obstruction of the flow of cAMP through the channels. This effect was larger when the transjunctional potential was positive, i.e., when the voltage gate of cx46 channel is activated. The Cl current elicited by cAMP at different transjunctional voltages thus was correlated with junctional conductance of the heterotypic cx46/43 channel, but with a shift to lower voltages because of the increase in open probability of the channel at low positive potentials.

Discussion

The results indicate that the voltage gate of gap junction channels changes the permeability of the channels depending on the size of the permeating molecules. Whereas the flux of small ions continues, the transit of larger molecules is impaired. This conclusion is based on two independent experimental methods, flux studies of fluorescent tracer molecules and of the second messenger cAMP.

The effect of voltage on cx46 channels at positive potentials involves two changes: first, a rectification process of single channel currents of unknown origin; second, the preferred dwelling of the channel in a subconductance state as also shown for other connexins (3, 10). Voltage-triggered subconductance states might be of physiological relevance by determining the flux of small molecules from cell to cell. However, previous studies on this issue have remained inconclusive. On the basis of single channel conductance measurements in different salt solutions, it has been concluded (5) that the "residual" state presents a stronger impairment for ion permeation than the fully open state. However, the discrimination between ions was moderate. The larger ions still permeated, although slightly less effectively than the smaller ions. Similarly, phosphorylation of cx43 gap junction channels has been reported to result in correlated changes of channel conductance and permeability for fluorescent tracer molecules (18). On the other hand, it has been

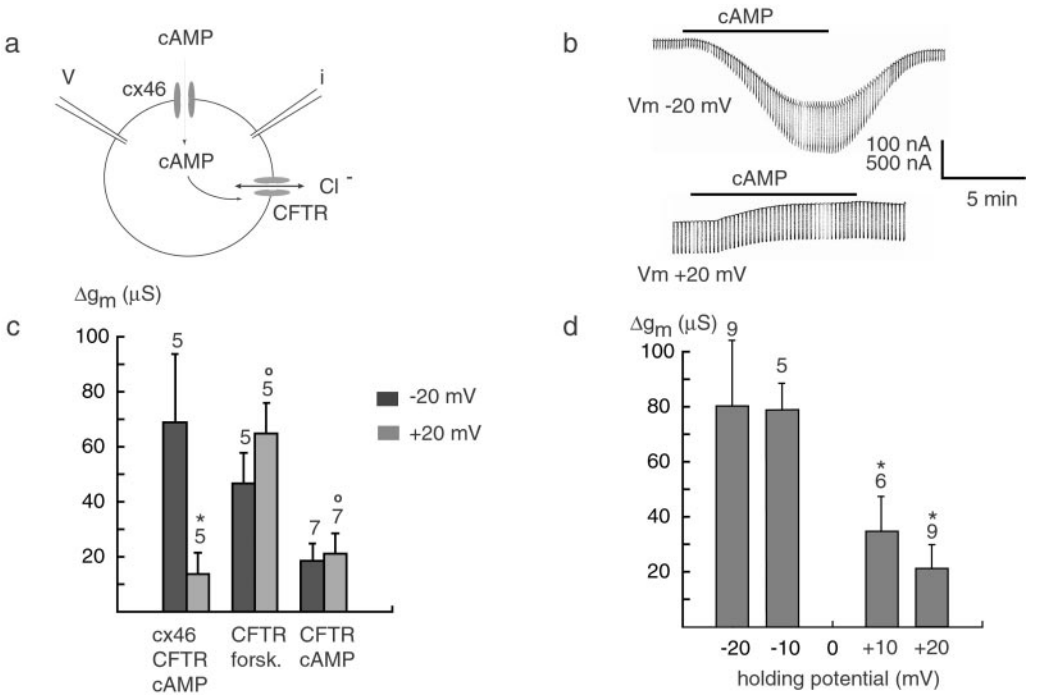

Fig. 4. Voltage-dependent flux of cAMP through cx46 hemichannels. (*a*) Oocytes coexpressing cx46 and CFTR were voltage clamped and exposed to extracellular cAMP at various holding potentials. (*b*) At −20 mV, cAMP triggered an inward current, and at +20 mV, an outward current consistent with a chloride current carried by CFTR (reversal potential −15 mV). Superimposed current pulses were used to determine membrane conductance. (*c*) Conductance changes for controls with oocytes expressing CFTR alone and exposed to forskolin or cAMP are shown. (*d*) Specific cAMP-induced membrane conductance as a function of holding potential. Data for *c* and *d* were obtained from different experimental sets. Means ± SE are plotted, and *n* is given above the bars. *, significantly different ($P < 0.05$); ○, not significantly different at the two voltages, ±20 mV.

argued, on the basis of dwell time distribution analysis, that subconductance states may not be physiologically relevant (6).

No correlation between conductance and permeability has also been found for gap junction channels formed by different connexins (19). Single channel conductances of gap junction channels cover a wide range, from 300 pS for cx37 gap junction channels to 14 pS for cx36 gap junction channels (20–22). Yet, the cutoff limit for the passage of fluorescent tracer molecules for most connexin channels is very similar, close to 1 kDa. In a perfectly cylindrical channel, conductance and permeability must be proportional unless binding domains within the pathway exist. In a noncylindrical channel, the permeation filter could comprise only a short segment of the channel, whereas the remainder of the channel, although of slightly larger diameter, could determine conductance because of its longer dimension. Gap junction channels seem to be noncylindrical (23, 24), thus a lack of correlation between conductance and permeability is not surprising for channels made of different connexins. In a noncylindrical channel, the voltage gate theoretically could change conductance without influencing permeability, or it could modify the permeability filter without altering conductance. However, the present data suggest that both the permeability filter and conductance are affected, which, however, does not preclude them to be separate entities.

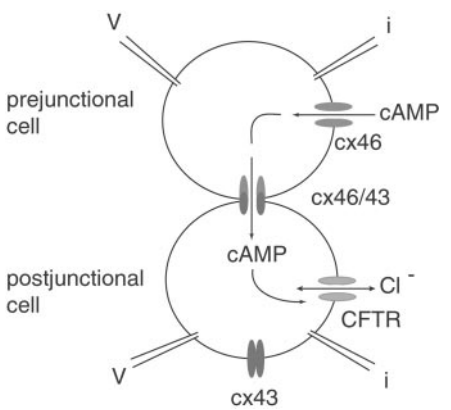

Fig. 5. Flux of cAMP through heterotypic cx46/cx43 gap junction channels. Pairs were formed of oocytes expressing cx46 (prejunctional) and coexpressing cx43 and CFTR (postjunctional). The prejunctional cell was always clamped at −20 mV to keep cx46 hemichannels open. The postjunctional cell was held at various potentials to generate the transjunctional potentials. The presumed flux of cAMP is indicated by arrows.

At positive potentials, not only does the channel dwell preferentially in the subconductance state, but also the less frequent excursions to the full open state have a smaller amplitude than at negative potentials, giving rise to rectification by a presently unknown mechanism. Thus, it is possible that the observed reduction of the flux of molecules through the channel is not only caused by the channel narrowing in the subconductance state but could also be caused by the rectification process. The present data do not allow a distinction between these possibilities. However, the observation that there is not total exclusion of the tracer molecules at positive potentials is consistent with exclusion when in the subconductance state and free or slowed passage when in the rectified state.

The voltage dependence of cx46 channels as related to the V_j gate is paradoxical; the channel conductance is reduced by rectification and by entering the subconductance state. Yet, the combined open probability in the fully open and subconductance states is increased over that at negative potential. Overall, this results in a moderate attenuation of macroscopic conductance so

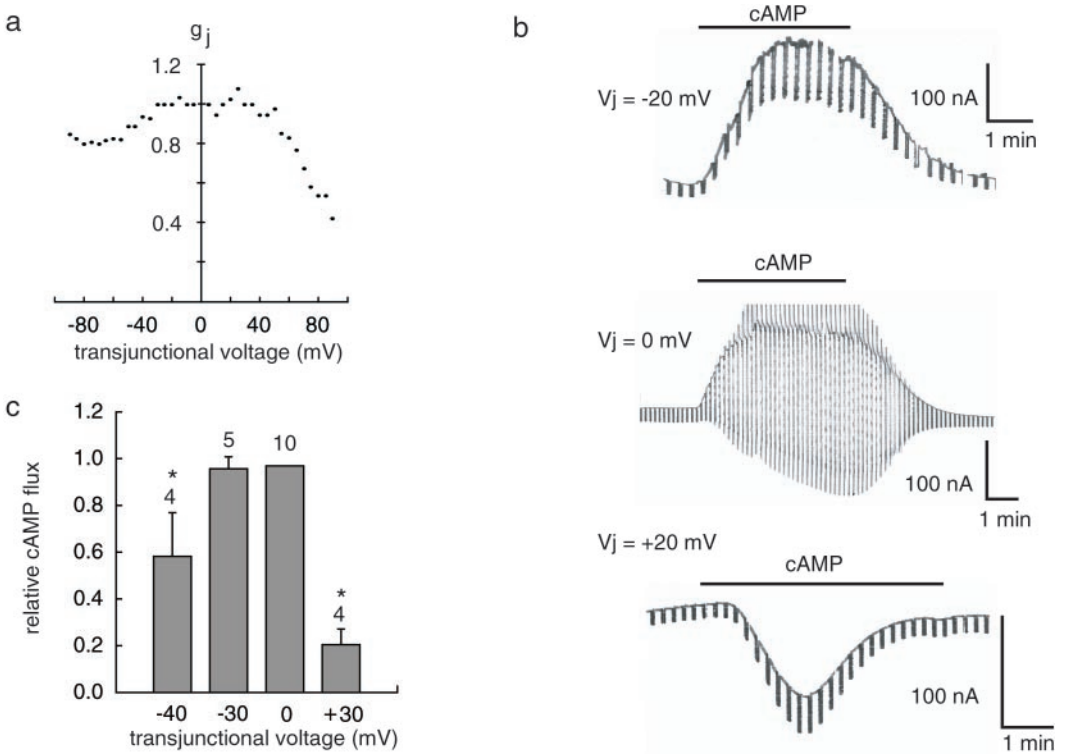

Fig. 6. Effect of transjunctional voltage on flux of cAMP through heterotypic cx46/cx43 gap junction channels. (*a*) Junctional conductance is plotted as a function of transjunctional voltage with the cx46-expressing prejunctional cell as reference point. (*b*) Membrane currents in the postjunctional cell induced by bath application of cAMP to a cell pair at the transjunctional voltages indicated are displayed. The prejunctional cell was always held at −20 mV; the postjunctional cell was held at 0, −20, or −40 mV to generate the transjunctional voltages indicated. Superimposed 5-mV voltage steps were used for determination of membrane conductance. (*c*) Relative cAMP flux is shown as specific membrane conductance induced by cAMP in postjunctional cells of heterotypic oocyte pairs normalized to the cAMP-induced membrane conductance at 0-mV transjunctional voltage. Means ± SE are plotted, and *n* is given above the bars. *, significantly different from value at 0 mV ($P < 0.01$).

that the electrical synchronization of cells will largely be undisturbed by the voltage gate. The physiological role of the voltage gate, therefore, might be the restriction of intercellular flow of second messengers and metabolites while preserving electrical continuity. Such a mechanism would prevent electrophoretic accumulation of charged molecules in parts of a tissue in the presence of an electrical field. An extreme case of such a scenario is found in cell injury, where the voltage gate would provide a "fast" block to the loss of compounds like ATP from healthy cells through gap junction channels into injured cell(s).

We thank Drs. K. Magleby and W. Nonner for valuable discussions and for critically reading the manuscript. This work was supported by National Institutes of Health Grant GM48610.

1. Bruzzone, R., White, T. W. & Paul, D. L. (1996) *Eur. J. Biochem.* **238,** 1–27.
2. Spray, D. C. (1996) *Clin. Exp. Pharmacol. Physiol.* **23,** 1038–1040.
3. Trexler, E. B., Bennett, M. V., Bargiello, T. A. & Verselis, V. K. (1996) *Proc. Natl. Acad. Sci. USA* **93,** 5836–5841.
4. Pfahnl, A. & Dahl, G. (1998) *Biophys. J.* **75,** 2323–2331.
5. Valiunas, V., Bukauskas, F. F. & Weingart, R. (1997) *Circ. Res.* **80,** 708–719.
6. Christ, G. J. & Brink, P. R. (1999) *Circ. Res.* **84,** 797–803.
7. Paul, D. L., Ebihara, L., Takemoto, L. J., Swenson, K. I. & Goodenough, D. A. (1991) *J. Cell Biol.* **115,** 1077–1089.
8. Ebihara, L. & Steiner, E. (1993) *J. Gen. Physiol.* **102,** 59–74.
9. Hopperstad, M. G., Srinivas, M. & Spray, D. C. (2000) *Biophys. J.* **79,** 1954–1966.
10. Hu, X. & Dahl, G. (1999) *FEBS Lett.* **451,** 113–117.
11. Dahl, G. (1992) in *Cell-Cell Interactions: A Practical Approach*, eds. Stevenson, B., Gallin, W. & Paul, D. (IRL, Oxford, U.K.), pp. 143–165.
12. Beyer, E. C., Paul, D. L. & Goodenough, D. A. (1987) *J. Cell Biol.* **105,** 2621–2629.
13. Bear, C. E., Duguay, F., Naismith, A. L., Kartner, N., Hanrahan, J. W. & Riordan, J. R. (1991) *J. Biol. Chem.* **266,** 19142–19145.
14. Levine, E., Werner, R., Neuhaus, I. & Dahl, G. (1993) *Dev. Biol.* **156,** 490–499.
15. Spray, D. C., Harris, A. L. & Bennett, M. V. (1981) *J. Gen. Physiol.* **77,** 77–93.
16. White, T. W., Bruzzone, R., Wolfram, S., Paul, D. L. & Goodenough, D. A. (1994) *J. Cell Biol.* **125,** 879–892.
17. Bukauskas, F. F., Bukauskiene, A., Bennett, M. V. & Verselis, V. K. (2001) *Biophys. J.* **81,** 137–152.
18. Kwak, B. R. & Jongsma, H. J. (1996) *Mol. Cell. Biochem.* **157,** 93–99.
19. Veenstra, R. D., Wang, H. Z., Beblo, D. A., Chilton, M. G., Harris, A. L., Beyer, E. C. & Brink, P. R. (1995) *Circ. Res.* **77,** 1156–1165.
20. Veenstra, R. D., Wang, H. Z., Beyer, E. C., Ramanan, S. V. & Brink, P. R. (1994) *Biophys. J.* **66,** 1915–1928.
21. Srinivas, M., Rozental, R., Kojima, T., Dermietzel, R., Mehler, M., Condorelli, D. F., Kessler, J. A. & Spray, D. C. (1999) *J. Neurosci.* **19,** 9848–9855.
22. Teubner, B., Degen, J., Sohl, G., Guldenagel, M., Bukauskas, F. F., Trexler, E. B., Verselis, V. K., De Zeeuw, C. I., Lee, C. G., Kozak, C. A., *et al.* (2000) *J. Membr. Biol.* **176,** 249–262.
23. Zhou, X. W., Pfahnl, A., Werner, R., Hudder, A., Llanes, A., Luebke, A. & Dahl, G. (1997) *Biophys. J.* **72,** 1946–1953.
24. Unger, V. M., Kumar, N. M., Gilula, N. B. & Yeager, M. (1999) *Science* **283,** 1176–1180.